Coincidence measurements of slow recoil ions with projectile ions in 42-MeV Ar^{q+}-Ar collisions

T. Tonuma and H. Kumagai
The Institute of Physical and Chemical Research (RIKEN), Wako-shi, Saitama 351-01, Japan

T. Matsuo
Department of Pathology, Tokyo Medical and Dental University, Yushima, Tokyo 113, Japan

H. Tawara
National Institute of Fusion Science, Nagoya 464-01, Japan
(Received 23 May 1989; revised manuscript received 19 July 1989)

Slow Ar recoil-ion production cross sections by projectiles of 1.05-MeV/amu Ar^{q+} ($q=4,6,8,10,12,14$) were measured using a projectile-ion–recoil-ion coincidence technique. The present results indicate that the average recoil ion charges $\langle i \rangle$ increase with increasing the incident projectile charge q and the number of the lost and captured electrons from and/or into projectiles, whereas the projectile charge-changing cross sections for loss ionization decrease steeply with increasing q for low-charge-state projectiles, and those for transfer ionization increase rapidly with increasing q for high-charge-state projectiles. For Ar projectiles with $q=10$, which corresponds to the equilibrium charge state of Ar projectiles at the present collision energy, the average recoil-ion charges are nearly the same in both loss and transfer ionization, and a pure ionization process plays a much more important role in producing highly charged recoil ions, in contrast to projectile electron loss or transfer processes, which play a role in other projectile charge states.

I. INTRODUCTION

Multielectron processes such as multiple ionization by charged particles are of continued interest, and it is known that highly charged, slow recoil ions are copiously produced by multiply charged, energetic heavy-ion impact. Coincidence measurements between projectile ion and recoil ion, therefore, provide useful information on the charge-state distributions or partial-ionization cross sections of the recoil ions correlated with the projectile final charge states, i.e., accompanied with either pure ionization without any change of the projectile charge, electron loss from or capture into the projectile ions. Experiments measuring such correlated charge-state distributions and partial-ionization cross sections of both collision partners with specified charges as well as related theoretical studies by fast heavy projectiles have been performed up to now.[1–12]

In the present work, we report on measurements of the partial production cross sections $\sigma^{i}_{q,q'}$ of recoil Ar^{i+} ions which are produced in the following collisions of partially ionized 1.05-MeV/amu Ar^{q+} projectile ions ($q=4,6,8,10,12,14$) with rare-gas Ar atoms to provide knowledge on mechanisms of multiple ionization of target atoms through pure ionization as well as of that accompanied simultaneously with multiple electron loss or capture of projectiles:

$$Ar^{q+}+Ar \rightarrow Ar^{q'+}+Ar^{i+}+(q'-q+i)e \quad (1)$$

for projectile charge change $k=q'-q=4,3,2,1,0,-1,-2,-3,-4$, i.e., $k>0$ ($q'>q$) corresponds to electron loss (so-called loss ionization) and $k<0$ ($q'<q$) to electron capture (transfer ionization).

II. EXPERIMENT

The experimental setup used is shown schematically in Fig. 1. The 1.05-MeV/amu Ar^{4+} or Ar^{6+} beams are provided with RIKEN heavy-ion linear accelerator. Ar^{q+} beams are selected with a switching magnet after passing through a carbon foil if necessary, collimated with 1-mm high and 0.4-mm wide aperture at the entrance of a target cell, and, then, directed into the gas-target cell which is differentially pumped. Projectile ions, a part of which may have changed their charge in a collision, are charge analyzed with an electrostatic deflection analyzer and detected with a position-sensitive parallel plate avalanche counter (PPAC). The distance between the target cell and the electrostatic charge analyzer is about 60 cm. On the other hand, slow recoil ions produced in collisions of projectile ions with gaseous target atoms are extracted perpendicularly to the projectile beam through a 3-mm-diam hole by the electric field between two parallel plates which are typically on potentials of +525 and +250 V, respectively. After passing another 3-mm-diam hole in the grounded plate and a subsequent drift tube, the recoil ions are detected with a channeltron detector located at about 15 cm from the target cell. The drift tube contains sets of an einzel lens and parallel plate deflectors to improve an overall transmission of the recoil ions. The recoil ions are charge analyzed in a time-of flight (TOF) spectrometer. The TOF spectrum of recoil ions is mea-

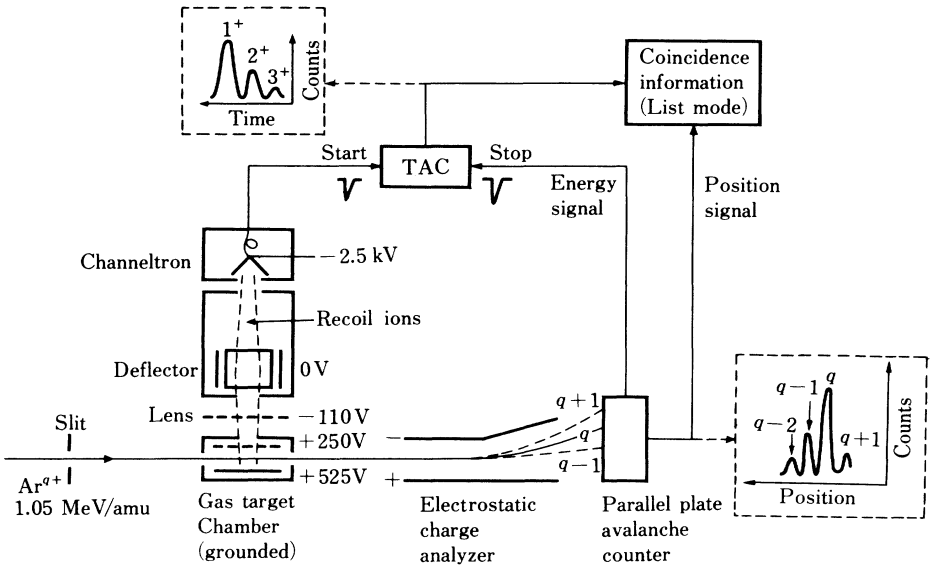

FIG. 1. Schematic experimental setup (not to scale).

sured by starting a time-to-amplitude converter (TAC) with signals produced by a recoil ion in the channeltron and stopping it with energy signals produced in the cathode plate of PPAC by projectile ions through a proper delay time. A projectile charge-state spectrum is recorded via position signals from the PPAC. On the basis of a list mode option, spectra which represent coincidence with a given window in the other spectrum can later be obtained.

Typical coincidence charge spectra of Ar recoil and Ar projectile ions in collisions of Ar^{10+} projectiles with Ar atoms with fully opened windows in both spectra are shown in Figs. 2(a) and 2(b). The coincidence count rate was about 10 Hz when the count rate of projectiles monitored by the PPAC was 8 kHz under the operating pressure of Ar targets of 7×10^{-4} Torr. Ar projectile charge spectrum taken in coincidence with all recoil ions [Fig. 2(b)] indicates that recoil ions are produced through either electron-capture ($q'=8$ and 9), pure ionization ($q'=10$), or electron-loss ($q'=11$ and 12) processes. It can be seen from the Ar recoil-ion charge spectrum [Fig. 2(a)] that Ar^{i+} recoil ions decrease rapidly as their charge state i becomes high.

When the windows in the projectile charge spectrum are set for the final charge states q' of Ar projectile ions, coincidence spectra of Ar^{i+} recoil ions show to be strongly correlated to the final charge states of the projectile ions. When the windows in the Ar^{i+} recoil charge spectrum are also set for the charge states i, spectra of Ar projectile ions show to significantly depend on the degree of multiple ionization of the recoil ions and the relative contribution of multiple electron processes of projectiles is clearly enhanced in producing higher charge recoil ions. Thus, the projectile charge distributions obtained in coincidence with recoil ions in each charge state could be used as crosscheck of the recoil-ion charge distribution.

It should be noted, however, that in coincidence measurements of Ar^{i+} recoil ions accompanied with electron-capture or -loss processes, recoil-ion yields with low charge, in particular, with $i=1$ and sometimes up to $i=3$, are enhanced through double collisions of the incident projectiles with Ar target atoms. As pointed out by Gray *et al.*,[1] a part of the projectile ions have changed inevitably their ionic charge due to collisions with the gas atoms outside the interaction region from which the recoil ions are extracted. The recoil ions could be coincident with these projectiles pre-and post-charge-changed outside the collision region through pure ionization since the production cross sections of singly charged recoil ions due to pure ionization are more than two orders of magnitude larger than those due to loss or transfer ionization. Background recoil ions produced through the double collisions are $N_q\sigma_{q,q'}t_1\sigma_{q',q'}t_0$ and $N_q\sigma_{q,q}t_0\sigma_{q,q'}t_2$ for pre- and post-charge-changed projectiles, respectively, and true recoil ions through single collisions are $N_q\sigma_{q,q'}t_0$, where N_q is the number of the incident projectiles with charge q, $\sigma_{q,q'}$ is the total charge-changing cross sections (as discussed later) of the projectile ions from q to q' charge state, $\sigma_{q',q'}$ and $\sigma_{q,q}$ are the pure ionization cross sections due to projectile with charge q' and q accompanied with target ionization (see Fig. 5), t_0, t_1, and t_2 are the target thickness of the interaction region, before and after the interaction region, respectively. Total thickness through the projectile beam line t is represent by $=t_0+t_1+t_2$. Thus, if the ratio of the target thickness (t_0) to total thickness (t), f, is given by $f=t_0/t$, the amount of background recoil ions observed in the coincidence measurement accompanying with the final charge states ($q'\neq q$) of the projectiles can be estimated from the relation

$$\frac{I_b}{I_{q,q'}}=\frac{1-f}{2}\frac{N_{q'}}{N_q}\frac{\sigma_{q,q}+\sigma_{q',q'}}{\sigma_{q,q'}}\ , \tag{2}$$

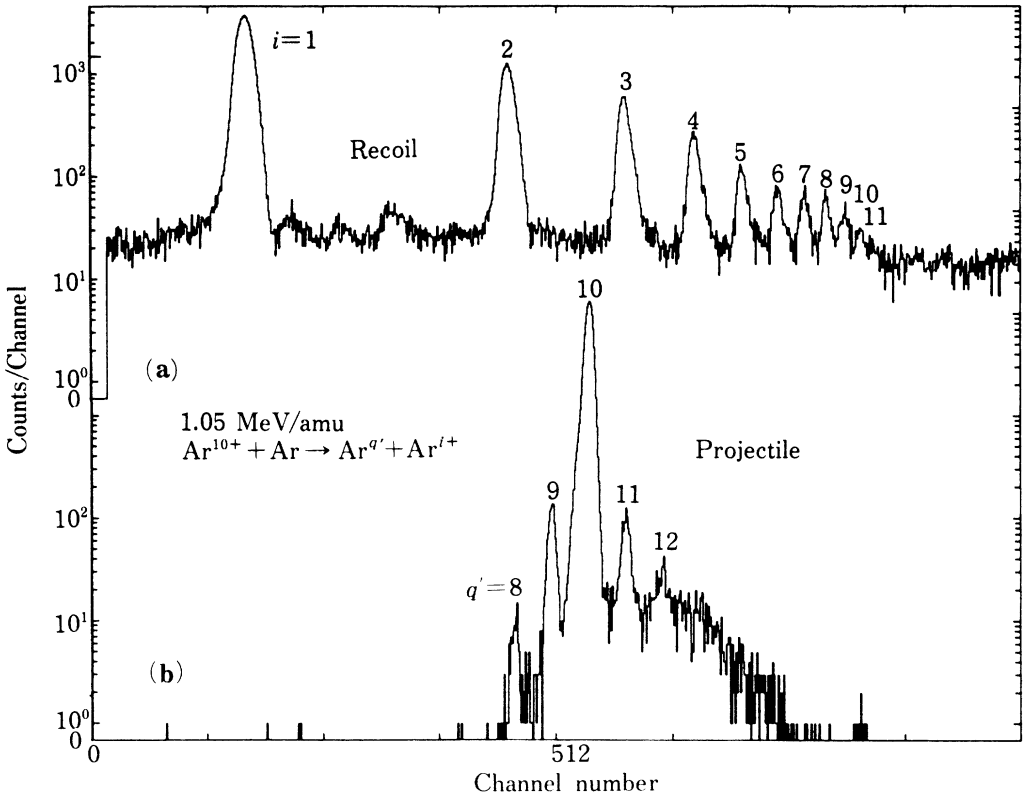

FIG. 2. Charge spectra of (a) Ar recoil ions and (b) Ar projectiles for 1.05-MeV/amu $Ar^{10+}+Ar$ collisions in the recoil-ion–projectile-ion coincidence measurement without projectile and recoil charge selection, respectively.

where I_b is the number of background recoil ions whose charge distributions are similar to those due to pure ionization, $I_{q,q'}$ is the total number of true recoil ions in coincidence with projectiles of the charge q', in other words, the number of coincident projectile ions counted by PPAC and $N_{q'}$ is given by $N_q\sigma_{q,q'}t$ and detected by PPAC without coincidence, but under the same target-gas pressure as in coincidence measurements. These ratios of $N_{q'}/N_q$ and f values (estimated to be 0.2 in the present work) depend on the apparatus and gas pressure distribution through the projectile beam line. However, $\sigma_{q',q'}$ cannot be determined simultaneously with other coincidence parameters but can be estimated through extrapolation or through separate measurements by the incident projectile with the charge state of q'. The contribution of this background due to the pre- and post-charge-changed projectiles depends on various collision parameters and the ratios of $I_b/I_{q,q'}$ are found to range from 10% to almost 100% in the present work.

We subtracted these backgrounds from recoil-ion spectra measured in coincidence with charge-changed projectiles, and thus determined "true" charge distributions accompanied with the electron-loss and -capture processes. The remaining uncertainties in the charge-state distributions are due to coincidence statistics, limited time resolution and difficulties in the integration of peaks. Absolute partial production cross sections $\sigma^i_{q,q'}$ of Ar^{i+} recoil ions for the collision process (1) were determined through these corrected coincidence data and normalization to the previous total cross sections.[13] Typical uncertainties of the cross sections $\sigma^i_{q,q'}$ estimated are given in Table I.

TABLE I. Typical uncertainties of cross sections $\sigma^i_{q,q'}$ determined. $\sigma^i_{q,q'}$ is in units of cm^2.

$-\log_{10}(\sigma^i_{q,q'})$	<16	16–17	17–18	18–19
uncertainties (%)	5	5–15	15–50	50–200

III. RESULTS AND DISCUSSION

Partial-ionization cross sections $\sigma^i_{q,q'}$ of Ar^{i+} recoil-ion production determined with the coincidence technique in collisions of 1.05-MeV/amu Ar^{q+} ($q=4-14$) projectiles are shown in Fig. 3 as a function of the recoil-ion charge i with the projectile final charge state q' (the number $k=q'-q$ represents that of the lost or captured electrons of projectiles) as a parameter. In all cases, the cross sections $\sigma^i_{q,q}$ ($k=0$) for pure ionization without any change of the projectile charge in the collisions decrease rapidly with increasing the recoil-ion charge i, indicating that low-charge-state recoil ions are mainly produced through collisions at large impact parameters. The production cross sections of the recoil ions in collisions where the

projectiles change their charge from q to q' are found to be strongly correlated to the projectile final charge q' and show quite different features compared with those due to pure ionization mentioned above.

Figure 4 shows the pure ionization cross sections $\sigma^i_{q,q}$ of Ar^{i+} recoil ions as a function of the recoil-ion charge i for the incident projectile charge $q=4-14$. In analyzing the pure ionization process we applied the independent electron approximation (IEA).[14] When the projectiles do not change their charge state q, the partial cross section $\sigma^i_{q,q}$ for i electron ionization in M shell of Ar atoms can be obtained by integrating over the impact parameters b,

$$\sigma^i_{q,q}=2\pi\int_0^\infty \binom{8}{i}[P_M(b)]^i[1-P_M(b)]^{8-i}b\,db\ , \tag{3}$$

where $\binom{8}{i}$ is the binomial coefficient, $P_M(b)$ is the ionization probability of a single M-shell electron at the impact parameter b and can be determined from the experimental data by assuming the following form:

$$P_M(b)=P_M(0)\exp(-b/r_M)\ , \tag{4}$$

which have been proved to be adequate for large impact parameters.[15] $P_M(0)$ and r_M can be determined by fitting (3) to the experimental data. The calculated results using

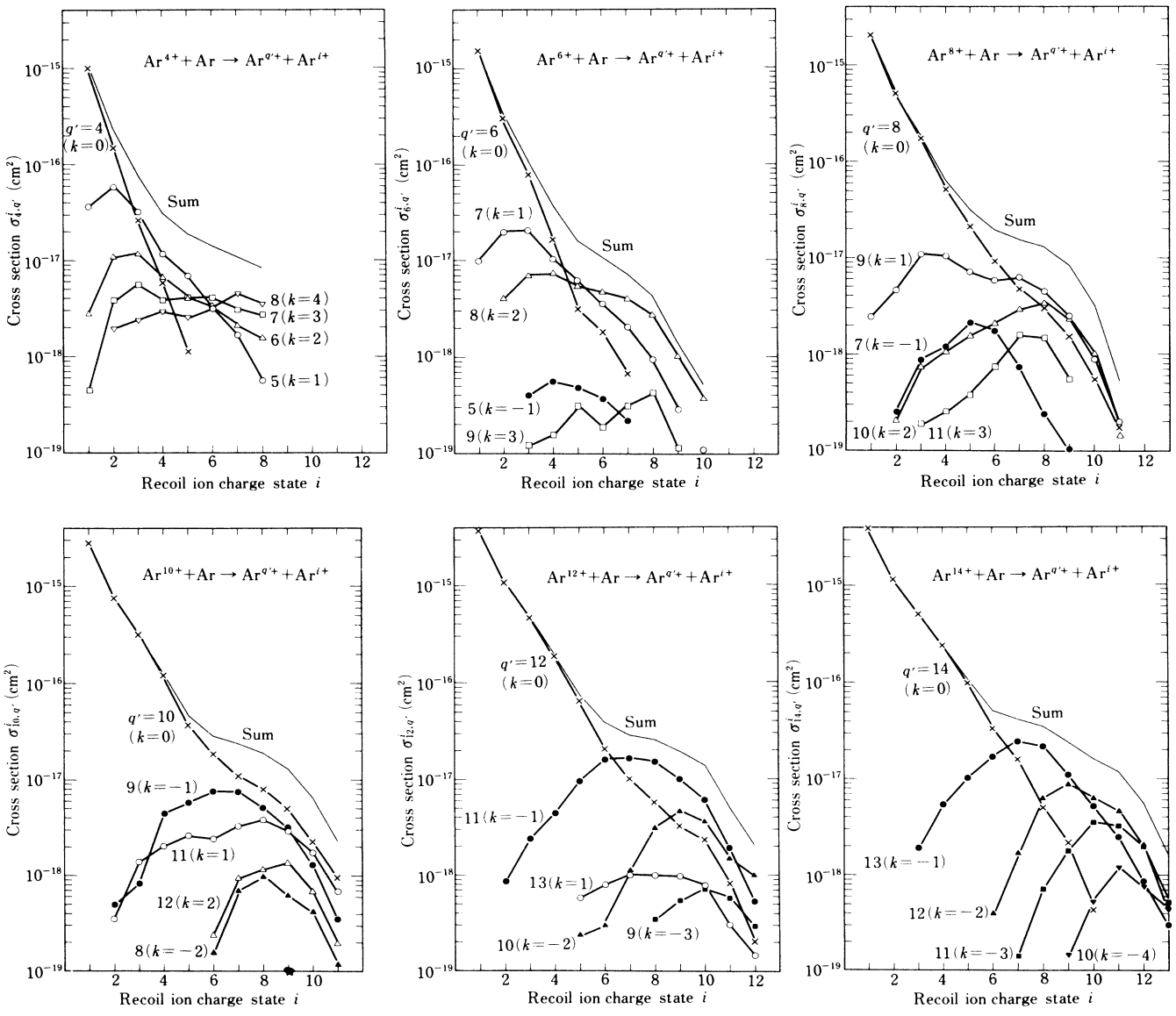

FIG. 3. Cross sections $\sigma^i_{q,q'}$ for pure ionization $q'=q\,(k=0)$, loss $q'>q\,(k>0)$ and transfer $q'<q\,(k<0)$ ionization in collisions of 1.05-MeV/amu Ar^{q+} ($q=4$, 6, 8, 10, 12, and 14) ions with Ar atoms. Sum denotes total cross sections summed over pure, loss, and transfer ionization processes. The lines are drawn to guide the eye.

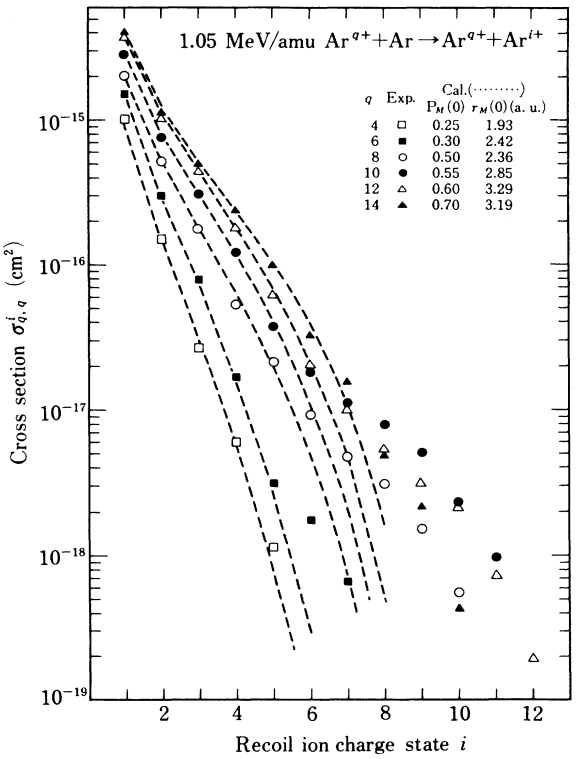

FIG. 4. Cross sections $\sigma^i_{q,q}$ for the production of recoil ions via pure ionization for 1.05-MeV/amu Ar^{q+} ($q=4$, 6, 8, 10, 12, 14) on Ar targets in comparison with a two-parameter fit in the IEA. The broken curves represent the results of the fitting procedure calculated with the parameters given in the figure.

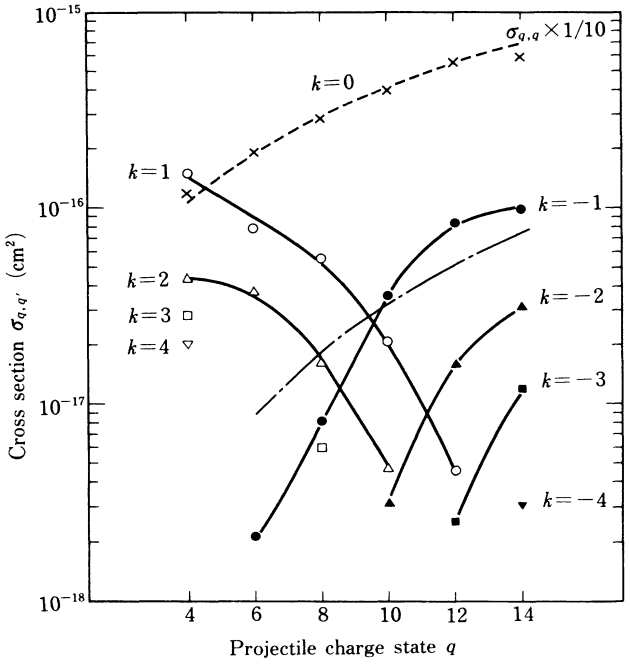

FIG. 5. Total projectile charge-changing cross sections $\sigma_{q,q'}$ for $Ar^{q+}+Ar \rightarrow Ar^{q'+}+Ar^{i+}$ ($q=4$–14). $k=0$ (×) represent pure ionization cross sections. $k=1$ (○), $k=2$ (△), $k=3$ (□), and $k=4$ (▽) denote one- up to four-electron-loss and $k=-1$ (●), $k=-2$ (▲), $k=-3$ (■), and $k=-4$ (▼) one- up to four-electron-capture cross sections. The solid curves are drawn to guide the eye. The dotted line for $k=0$ and the dash-dotted line for $k=-1$ are explained in the test.

these values of $P_M(0)$ and r_M thus determined are plotted with the dotted lines and compared with the experimental data in Fig. 4.

This model is found to give a good description of the present data $\sigma^i_{q,q}$ in low-charge recoil ions from $i=1$ up to $i=5$–6 in all $Ar^{q+}+Ar$ collisions investigated. However, it is clearly seen in Fig. 4 that the present calculations applied only for the outermost shell, that is, M-shells of Ar atoms underestimate the cross sections for the production of higher charge-state recoil ions. This result may suggest that highly charged Ar recoil ions due to pure ionization are produced not only through direct multiple ionization of the outermost shell, but also through inner-shell ionization (L shell in this particular case) followed by Auger electron emission and vacancy cascade, resulting the enhancement of higher charge ions.

Total cross sections $\sigma_{q,q'}$ summed over partial cross section $\sigma^i_{q,q'}$ of Ar recoil ions with different charge i, namely, total charge-changing cross sections of projectiles from q to q' including all ionization states of target atoms is written as follows:

$$\sigma_{q,q'}=\sum_{i=1}\sigma^i_{q,q'} . \tag{5}$$

Figure 5 shows the cross sections $\sigma_{q,q'}$ as a function of the incident projectile charge q. Total cross sections for pure ionization ($k=0$) $\sigma_{q,q}$ (crosses in the figure) increase with increasing projectile charge q. Total cross sections of pure ionization are approximated with $\sigma_{q,q}=Aq^a$, where A and a denote the fitting parameters. The determined values $a=1.5$ and $A=1.3\times10^{-16}$ cm², which reproduce well the present data as displayed with a dotted line in the figure, can be compared with the values $a=1.7$ and $A=1.2\times10^{-16}$ cm² obtained in the net ionization cross sections which had been previously measured under the same collision system as in the present work,[16] indicating that the net ionization cross sections are dominated by the pure ionization process.

As expected, single and multiple electron-loss processes ($k>0$) are found to be dominant for low-charge-state projectiles and their cross sections decrease steeply with increasing the projectile charge q, whereas electron capture into projectiles ($k<0$) is dominant for high-charge-state projectile and the cross sections increase with increasing q. Single-electron-capture cross sections ($k=-1$) calculated, based on the Nikolaev empirical formula,[17] are shown with the dash-dotted line and show slower increase than the present experimental data. The ratios of double-to-single–electron-capture cross sections range from 0.1 to 0.3 in the present data which are comparable to that (about 20%) found in the charge-changing cross-section measurements by other investigators.[18] From this figure, electron-loss cross sections are found to become equal to electron-capture cross sections at about

$q=10$ for both single- and double-electron processes which seems to correspond roughly to the equilibrium charge $\bar{q}$ of 1.05-MeV/amu Ar projectiles in collisions with Ar gas targets. Indeed this number agrees well with $\bar{q}=10.3$ derived from an empirical formula by Dmitriev *et al.*[19] and $\bar{q}=10.2$ by Betz *et al.*[20]

By introducing the average charge $\langle i \rangle$ of Ar^{i+} recoil ions produced in a specific collision process of (1), general trends on the degree of target ionization in the present data can be easily visualized. The average charge $\langle i \rangle_{q,q'}$ is obtained from the measured cross sections $\sigma^{i}_{q,q'}$ through

$$\langle i \rangle_{q,q'} = \sum_{i=1} i\sigma^{i}_{q,q'}/\sigma_{q,q'} , \tag{6}$$

where $\sigma_{q,q'}$ is the projectile changing cross sections represented by Eq. (5). Figure 6 shows $\langle i \rangle_{q,q'}$ as a function of the incident projectile charge q with the number $k=q'-q$ of the lost and captured electrons as a parameter. The average recoil-ion charges $\langle i \rangle_{q,q}$ for pure ionization ($k=0$) increase only slightly from 1.19 to 1.62 with increasing the projectile charge q from 4 to 14, indicating that the recoil ions of low-charge states, in particular, singly charged ions, are produced most dominantly in the pure ionization process. In electron-loss and -capture processes, the average charge $\langle i \rangle$ increases significantly with projectile charge. It is noteworthy that $\langle i \rangle$ for electron-capture processes $k=-2$ and -1 is different roughly by a two-unit charge, suggesting that the process with $k=-2$ involves the inner-shell ionization or excitation followed by Auger electron emission. On the other hand, $\langle i \rangle$ for electron-loss processes $k=2$ and 1 differs roughly by unit, indicating that the process with $k=2$ and also $k=3$–4 involves an additional electron ionization in the same shell as that in $k=1$. It can be noted, however, that for higher q the difference tends to increase with increasing q, suggesting that again the inner-shell electron process contributes to the production of higher charge recoil ions.

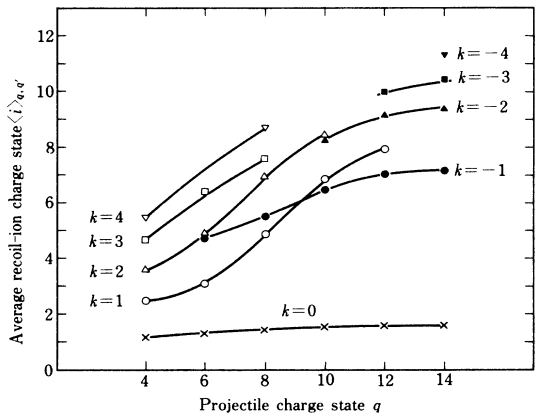

FIG. 6. Average recoil-ion charges $\langle i \rangle$ vs the projectile charge state q in $Ar^{q+}+Ar \rightarrow Ar^{q'+}+Ar^{i+}$ collisions. The number k is a parameter with the following symbols assigned: $k=0$ (×), $k=1$ (○), $k=2$ (△), $k=3$ (□), $k=4$ (▽), $k=-1$ (●), $k=-2$ (▲), $k=-3$ (■), and $k=-4$ (▼). The lines are drawn to guide the eye.

It would be interesting to compare the average recoil-ion charge $\langle i \rangle_{q,q'}$ with the projectile charge-changing cross sections $\sigma_{q,q'}$. For loss ionization ($k>0$) processes, the average charge state $\langle i \rangle_{q,q'}$ shifts toward higher values with increasing projectile charge q and the number k of the lost electrons of the projectile, whereas the corresponding cross sections $\sigma_{q,q'}$ decrease steeply with increasing q and k. This fact suggests that the projectiles have to penetrate deeply into target atoms in order to produce highly charged recoil ions through the loss ionization process. On the other hand, for the transfer ionization ($k<0$) process, the average recoil-ion charges $\langle i \rangle_{q,q'}$ as well as the electron-capture cross sections $\sigma_{q,q'}$ increase with the projectile charge q. The present data, as described above, suggest that the average charges of Ar recoil ions for double-electron capture ($k=-2$) is found to shift higher by two charge units, compared with those in the single capture and capture of three or four electrons increases only one charge unit for each electron capture. Similar shifts of maximum positions in charge distributions between single- and double-electron processes of projectiles have been already observed by others.[6,7] Levin *et al.*[7] have explained these shifts by assuming that, in addition to M-shell ionization with binomial distributions, one or two L-shell ionizations followed by vacancy cascades is more probable instead of almost complete M-shell ionization. Capture of three or four electrons into projectiles results in only incremental target ionization of one or two more M-shell electrons because the number of M electrons which survive the initial interaction are depleted through vacancy cascades so that further vacancy multiplication becomes less efficient. It can be expected, indeed, from the present double-electron-capture cross sections and the projectile velocity in the present collision energy comparable to the L-shell electron orbital velocity, that the projectile penetrates into the vicinity of the L-shell orbit and captures an L-shell electron of Ar target atoms, resulting in production of L-shell vacancy. It should be noted that the cross sections for K-shell ionization and/or excitation through either direct process or quasimolecular formation are estimated to be the order of 10^{-19} cm^2 if the projectiles have no K-shell vacancies[21] as in the present case and, then, K shell plays a minor role in the present collision system.

As seen in Fig. 6, the average charges of recoil ions $\langle i \rangle_{q,q'}$ at $q=10$, where already mentioned above, the electron-loss and -capture cross sections of the projectile are roughly equal, seem to be independent whether they are produced through electron-loss or -capture ionization: $\langle i \rangle_{10,11}=6.85$ and $\langle i \rangle_{10,9}=6.46$ accompanying with single-electron-loss and -capture whereas $\langle i \rangle_{10,12}=8.44$ and $\langle i \rangle_{10,8}=8.28$ with double-electron loss and capture from and/or into the projectile, respectively. These results suggest that the collisions through loss and transfer ionization should occur at comparable impact parameters, resulting in the production of highly charged recoil ions with the almost same average charges. The average charges $\langle i \rangle_{q,q'}$ for single-electron loss and cap-

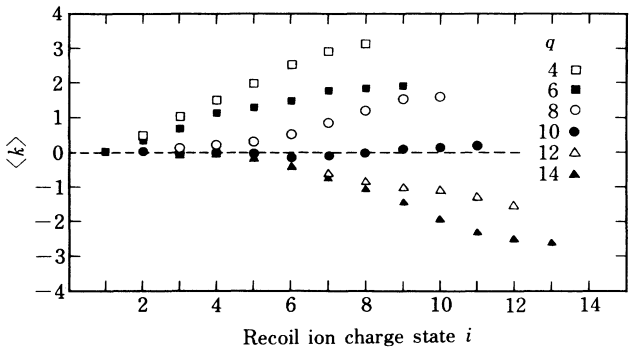

FIG. 7. Average projectile charge change $\langle k \rangle$ for $Ar^{q+} + Ar \rightarrow Ar^{q'+} + Ar^{i+}$ collisions with $k = q' - q$ vs the recoil-ion charges i as a parameter of the projectile charge state $q = 4$, 6, 8, 10, 12, and 14.

ture except for that at $q = 10$ are significantly different; for example, $\langle i \rangle_{6,7} = 3.08$ and $\langle i \rangle_{6,5} = 4.76$ at $q = 6$, $\langle i \rangle_{12,13} = 7.92$ and $\langle i \rangle_{12,11} = 7.02$ at $q = 12$, whereas the charge-changing cross sections $\sigma_{q,q'}$ for $k = 1$ are quite different from those for $k = -1$, i.e, $\sigma_{6,7} \gg \sigma_{6,5}$ at $q = 6$ and $\sigma_{12,13} \ll \sigma_{12,11}$ at $q = 12$. This indicates a trend that the smaller charge-changing cross sections of the projectiles give the higher average charges of recoil ions. In fact, deep penetration in electron capture for $q = 6$ and in electron loss for $q = 12$ results in production of higher charged recoil ions but in smaller cross sections.

General features of the production of recoil ions correlated with the projectile charge change can be easily visualized in another way by introducing the average charge change of projectiles $\langle k \rangle$,

$$\langle k \rangle = \sum_k k F_k \ , \tag{7}$$

where F_k is the fraction of projectiles whose charge changes by k and can be determined from the projectile charge spectrum as in Fig. 2(b). Figure 7 shows $\langle k \rangle$ as a function of the recoil-ion charge state i with the incident projectile charge q as a parameter. It is seen that singly charged recoil ions ($i = 1$) are produced dominantly through pure ionization ($k = 0$) which is independent of the projectile charge. The ionization processes producing highly charged recoil ions clearly depend on the projectile charge. The fact that the average charge change $\langle k \rangle$ for the projectile charge $q = 4$–8 are positive and increase with increasing recoil-ion charge i, indicates that highly charged recoil ions are produced mainly through multielectron-loss ionization ($k > 0$) of the projectiles and the contribution of loss ionization increases for higher recoil ion charge and lower projectile charge. On the other hand, for $q = 12$ and 14, $\langle k \rangle$ are negative and decrease with increasing i and recoil ions are produced mainly through transfer ionization ($k < 0$), and the contribution of transfer ionization increases with increasing recoil and projectile charge. On the contrary, for the projectile charge $q = 10$ corresponding roughly to the equilibrium charge, $\langle k \rangle$ is roughly zero, indicating that the contribution of both loss and transfer ionization is similar and minimal and, moreover, the pure ionization plays an important role in producing highly charged recoil ions

IV. CONCLUSIONS

We have measured projectile initial and final charge-state-dependent cross sections for the production of recoil ions in 1.05-MeV/amu $Ar^{q+} + Ar$ collision system with a projectile-ion–recoil-ion coincidence technique. It is clearly shown that high-charge recoil ions are produced mainly through electron loss for low initial charge of projectiles. On the other hand, for high projectile charge, recoil ions are produced mainly through the electron-transfer process.

It is interesting to note that electron-loss and -capture cross sections for both single- and double-electron processes of projectiles become roughly equal at about $q = 10$, which should be compared with the equilibrium charge of Ar projectiles in the present collision energy. There the average recoil-ion charges due to both electron-loss and -capture processes are also roughly equal and pure ionization is found to play an important role in the production of highly charged recoil ions. It is found that the comparison of the average recoil-ion charges with the charge-changing cross sections of projectile ions provides qualitative as well as quantitative information on the production of highly charged recoil ions accompanied with multiple-electron processes in projectiles.

It should be also noted that up to now, very few experimental as well as theoretical investigations have been devoted toward studying the mechanisms of recoil ion production when the loss ionization of projectiles with a number of the screening electrons is accompanied simultaneously. In order to fully understand such a multiple ionization of recoil target atoms, further accumulation of experimental data similar to the present work is required as well as investigations of related topics such as the impact-parameter dependence which has been already studied by Olson[9] and Horbatsch[10,11] to some extent.

ACKNOWLEDGMENTS

The authors would like to thank Dr. H. Shibata for joining a part of the present work and also to acknowledge the partial support of the Ministry of Education, Science and Technology, Japan.

[1]T. J. Gray, C. L. Cocke, and E. Justiniano, Phys. Rev. A **22**, 849 (1980).

[2]H. Damsgaard, H. K. Haugen, P. Hvelplund, and H. Knudsen, Phys. Rev. A **27**, 112 (1983).

[3]S. Kelbch, H. Schmidt-Böcking, J. Ullrich, R. Schuch, E. Justiniano, M. Ingwersen, and C. L. Cocke, Z. Phys. A **317**, 9 (1984).

[4]A. Müller, B. Schuch, W. Groh, E. Salzborn, H. F. Beyer, P.

H. Mokler, and R. E. Olson, Phys. Rev. A **33**, 3010 (1986).
[5]J. Ullrich, K. Bethge, S. Kelbch, W. Schadt, H. Schmidt-Böcking, and K. E. Stiebing, J. Phys. B **19**, 437 (1986).
[6]A. Müller, B. Schuch, W. Groh, and E. Salzborn, Z. Phys. D **7**, 251 (1987).
[7]J. C. Levin, C.-S. O. H. Cederquist, C. Biedermann, and I. A. Sellin, Phys. Rev. A **38**, 2674 (1988).
[8]H. Bery, R. Dorner, C. Kelbch, S. Kelbch, J. Ullrich, S. Hagmann, P. Richard, H. Schmidt-Böcking, A. S. Schlachter, M. Prior, H. J. Crawford, J. M. Engelage, I. Flores, P. H. Loyd, J. Pedersen, and R. E. Olson, J. Phys. B **21**, 3929 (1988).
[9]R. E. Olson, J. Phys. B **12**, 1843 (1979).
[10]M. Horbatsch, Z. Phys. D **1**, 337 (1986).
[11]M. Horbatsch and R. M. Dreizler, Z. Phys. D **2**, 183 (1986).
[12]I. Ben-Itzhak, T. J. Gray, J. C. Legg, and J. H. McGuire, Phys. Rev. A **37**, 3685 (1988).
[13]T. Tonuma, H. Shibata, S. H. Be, H. Kumagai, M. Kase, T. Kambara, I. Kohno, A. Ohsaki, and H. Tawara, Phys. Rev. A **33**, 3047 (1986).
[14]J. H. McGuire and L. Weaver, Phys. Rev. A **16**, 41 (1977).
[15]P. H. Mokler and H. D. Liesen, in *Progress in Atomic Spectroscopy,* edited by H. F. Berger and H. Kleinpoppen (Plenum, New York, 1983), p. 321.
[16]S. H. Be, T. Tonuma, H. Kumagai, H. Shibata, M. Kase, T. Kambara, I. Kohno, and H. Tawara, J. Phys. B **19**, 1771 (1986).
[17]V. S. Nikolaev, L. N. Fateeva, I. S. Dmitriev, and Ya. A. Teplova, Zh. Eksp. Teor. Fiz. **33**, 306 (1957) [Sov. Phys.—JETP **6**, 239 (1957)].
[18]H. D. Betz, in *Methods of Experimental Physics: Atomic Physics (Accelerators)* edited by P. Richard (Academic, New York, 1975).
[19]I. S. Dmitriev and V. S. Nikolaev, Zh. Eksp. Teor. Fiz. **47**, 615 (1964) [Sov. Phys.—JETP **20**, 409 (1965)].
[20]H. D. Betz, G. Hortig, E. Leischner, Ch. Schmelzer, B. Stadler, and J. Weihrauch, Phys. Lett. **22**, 643 (1963).
[21]L. M. Wintes, J. R. McDonald, M. D. Mrown, T. Chiao, L. D. Ellsworth, and E. W. Pettus, Phys. Rev. A **8**, 1835 (1973); J. R. McDonald, M. D. Brown, S. J. Czuchlewski, L. M. Winters, R. Laubert, I. A. Sellin, and J. R. Mowat, *ibid.* **14**, 1977 (1976); W. E. Meyerhof, *ibid.* **10**, 1005 (1974).